REPORTS

PLANETARY SCIENCE

Dawn arrives at Ceres: Exploration of a small, volatile-rich world

C. T. Russell,[1]* C. A. Raymond,[2] E. Ammannito,[1] D. L. Buczkowski,[3] M. C. De Sanctis,[4] H. Hiesinger,[5] R. Jaumann,[6] A. S. Konopliv,[2] H. Y. McSween,[7] A. Nathues,[8] R. S. Park,[2] C. M. Pieters,[9] T. H. Prettyman,[10] T. B. McCord,[11] L. A. McFadden,[12] S. Mottola,[6] M. T. Zuber,[13] S. P. Joy,[1] C. Polanskey,[2] M. D. Rayman,[2] J. C. Castillo-Rogez,[2] P. J. Chi,[1] J. P. Combe,[11] A. Ermakov,[13] R. R. Fu,[14] M. Hoffmann,[8] Y. D. Jia,[1] S. D. King,[15] D. J. Lawrence,[3] J.-Y. Li,[10] S. Marchi,[16] F. Preusker,[6] T. Roatsch,[6] O. Ruesch,[12] P. Schenk,[17] M. N. Villarreal,[1] N. Yamashita[10]

On 6 March 2015, Dawn arrived at Ceres to find a dark, desiccated surface punctuated by small, bright areas. Parts of Ceres' surface are heavily cratered, but the largest expected craters are absent. Ceres appears gravitationally relaxed at only the longest wavelengths, implying a mechanically strong lithosphere with a weaker deep interior. Ceres' dry exterior displays hydroxylated silicates, including ammoniated clays of endogenous origin. The possibility of abundant volatiles at depth is supported by geomorphologic features such as flat crater floors with pits, lobate flows of materials, and a singular mountain that appears to be an extrusive cryovolcanic dome. On one occasion, Ceres temporarily interacted with the solar wind, producing a bow shock accelerating electrons to energies of tens of kilovolts.

Ceres was discovered by G. Piazzi on 1 January 1801, between the orbits of Mars and Jupiter at the heliocentric distance expected for the missing planet predicted by the Titius-Bode law (*1*). The fourth asteroid to be discovered, Vesta, was explored by the Dawn spacecraft from June 2011 to August 2012 (*2*). Whereas Vesta is associated with a family of vestoids and the howardite-eucrite-diogenite (HED) achondrites, Ceres is not associated with a family of asteroids or known meteorites. Consequently, unlike at Vesta, there are few geochemical clues to its composition and few hypotheses to be tested. Remote sensing with telescopes at 1 astronomical unit (AU) and probing with Earth-based radar have revealed little about this low-albedo body, although they do indicate a clay-like surface (*3*, *4*). Hubble Space Telescope (HST) observations provided a size and shape (*5*) that suggested a geologically differentiated body. The size, combined with a mass estimate based on its gravitational interaction with Mars (*6*), indicated that Ceres' average density was about 2100 kg·m^{-3}. Thermodynamic models (*7*, *8*) predicted from this estimated bulk density that Ceres contained 17 to 27% free water by mass, and therefore it likely had fractionated into a silicate core and a water-rich mantle. These inferences of a "wet" dwarf planet were supported by a possible detection of OH with the International Ultraviolet Explorer (*9*), but could not be verified from ground-based telescopes. More recently, the Herschel Space Observatory confirmed the presence of water vapor molecules at Ceres with a source rate of about 6 kg·s^{-1} (*10*). The possible presence of ammonium-bearing minerals (*11*) and brucite mixed with carbonate (*12*) on Ceres' surface had been suggested from telescopic spectra. Global infrared spectra obtained on Dawn's approach to Ceres, without the interference of the Earth's atmospheric water and methane, confirmed a match to ammoniated phyllosilicates (*13*).

Dawn entered orbit about Ceres on 6 March 2015 and maneuvered into its rotational characterization orbit at a 14,000-km radius in which it operated from 23 April to 9 May. A 4900-km survey orbit followed from 6 to 30 June, and a 1950-km radius, high-altitude mapping orbit from 17 August to 23 October. Its final orbit, low-altitude mapping at a radius of 850 km, was entered on 16 December 2015. A refined Ceres coordinate system is anchored by a small crater at 0° longitude and 2°S, named Kait (*14*). Ceres longitudes increase eastward, in the direction of rotation (*15*). Using methods described in the supplementary materials, we find that Ceres rotates about an axis with a right ascension of 291.42° ± 0.01° and a declination of 66.76° ± 0.02° with a period of 9.074170 ± 0.000001 hours. The declination is a change of nearly 8° from that obtained earlier by HST (*5*). The angle between Ceres' orbital pole and rotational pole, its obliquity, is 4°. Ceres' mass, determined from Dawn's orbital parameters, is (9.384 ± 0.001) × 10^{20} kg, similar to earlier estimated values (*6*). Its triaxial elliptical dimensions are 483.1 by 481.0 by 445.9, all ± 0.2 km for a geometric mean radius of 469.7 km, similar to the recent value obtained at the Keck Observatory with adaptive optics (*16*). The resulting mean density is 2162 ± 3 kg m^{-3} (see methods section in supplementary materials).

Initial observations revealed Ceres to have a heavily cratered dark surface with a geometric albedo of ~0.09 (*17*), but punctuated with widely distributed small, bright deposits with one large complex of very bright areas on the floor of the 92-km Occator crater (*18*), near 239° longitude and 22°N latitude (Fig. 1). The location and distribution of the bright material in the crater floor suggest the presence of several subsurface conduits of bright material with differing fluences rather than emplacement due to multiple impacts, although mobilization could be associated with an impact. The material is in low-lying areas of the crater floor, albeit not in the lowest part of the crater floor. Visible colors of the bright material show a distinct spectral character (*18*). Infrared spectra of the bright material show the presence of abundant carbonates (*19*) and no detectable water-ice bands. These properties are consistent with cryovolcanism, delivering materials produced at depth to the surface, but not within the time frame of water-ice stability on the surface. The ubiquitous distribution of ammoniated phyllosilicates across Ceres requires a global mixing process (*20*).

A 4-km-high mountain, Ahuna Mons, is shown in Fig. 2, the faces of its flanks exhibiting bright streaks. The morphologically fresh appearance of the flanks, the general lack of debris at their base, and the scarcity of craters on the dome point to a geologically young feature. The overall morphometry and the morphologies on the mountain summit have been attributed to a formation through viscous extrusion. An accompanying paper (*21*) proposes that the extrusive event was enabled by the presence at depth of a cryomagma involving salts of low eutectic temperatures.

Although heavily cratered, as are other airless bodies in the solar system, the surface of Ceres differs from those of other bodies of similar size. Figure 3 compares similarly sized typical craters on Vesta, Ceres, and Rhea, an icy moon of Saturn. The vestan crater is excavated in deep regolith and is bowl-shaped with an almost circular

[1]Earth Planetary and Space Sciences, University of California, Los Angeles, 603 Charles Young Drive, Los Angeles, CA 90095-1567, USA. [2]Jet Propulsion Laboratory, California Institute of Technology, Pasadena, CA 91109-8099, USA. [3]Johns Hopkins University Applied Physics Laboratory, Laurel, MD 20723-6099, USA. [4]Istituto di Astrofisica e Planetologia Spaziali, Istituto Nazionale di Astrofisica, 00133 Roma, Italy. [5]Institut für Planetologie, 48149 Münster, Germany. [6]Deutsches Zentrum fur Luft-und Raumfahrt, Institute of Planetary Research, 12489 Berlin, Germany. [7]Department of Earth and Planetary Sciences, University of Tennessee, Knoxville, TN 37996-1410, USA. [8]Max-Planck-Institut für Sonnensystemforschung, Justus-von-Liebig-Weg 3, 37077 Göttingen, Germany. [9]Brown University, Department of Earth, Environmental, and Planetary Sciences, Providence, RI 02912, USA. [10]Planetary Science Institute, Tucson, AZ 85719, USA. [11]The Bear Fight Institute, Winthrop, WA 98862, USA. [12]NASA Goddard Space Flight Center, Greenbelt, MD 20771, USA. [13]Massachussetts Institute of Technology, Cambridge, MA 02139, USA. [14]Lamont-Doherty Earth Observatory, Columbia University, Palisades, NY 10968, USA. [15]Virginia Tech, Geosciences, Blacksburg, VA 24061, USA. [16]Southwest Research Institute, Boulder, CO 80302, USA. [17]Lunar and Planetary Institute, Houston, TX 77058, USA.
*Corresponding author. Email: ctrussell@igpp.ucla.edu

rim; the rhean crater is excavated in hard, cold ice and has an irregularly shaped rim and an irregular floor and steep walls. Although the cerean crater also has an irregularly shaped rim, an irregular floor, and steep walls, there is a large region of smooth floor, suggesting the production of impact melt. These craters illustrate that the surface of Ceres is intermediate in strength between that of rocky Vesta and icy Rhea. Impact melt was not observed at Vesta in appreciable amounts (*22*, *23*); thus, because of similar expected impact velocities, this observation is consistent with the presence of ice and other volatiles in the rocky crust of Ceres (*24*). However, if ice dominated the cerean crust, then craters would be expected to relax on short time scales (*25*). Because the crater size-frequency distribution (*26*) indicates that little relaxation occurs at the shorter wavelengths, the fractional content of ice in the crust must be limited. A mixture of ice and rock (or salt hydrates) could have the strength to retain these craters over billions of years (*27*). Ceres' crater distribution (*26*) and geomorphology (*24*) support the inference of a mechanically strong crust and upper mantle composed of rock, ice, and possibly salt hydrates that is periodically mobilized to produce extrusive features such as Ahuna Mons, as well as flow features and bright deposits. To date, only one area in the Oxo crater, centered at 359.7°E and 42.2° N, shows evidence of H_2O-rich surface materials (*28*). Exposed ice on Ceres at such mid-latitudes should become undetectable within hundreds of years, implying that Oxo has an active or recently exposed surface.

The gravity measurements described in the supplementary materials indicate that Ceres is close to hydrostatic equilibrium, with evidence for a denser core and low-density mantle and crust. The observed lack of large basins (*24*) and the subdued power at long wavelengths in Ceres' topographic spectrum indicate efficient relaxation of the topography at depth in the lower mantle, whereas the retention of small- to medium-sized craters points toward a strong upper mantle or lithosphere.

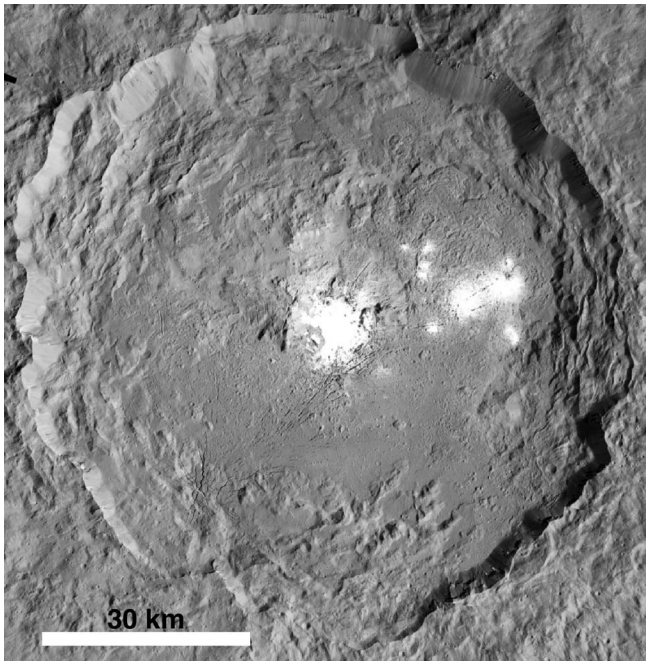

Fig. 1. Occator crater (239.3°E, 19.8°N) imaged from 1500-km altitude in a panchromatic filter. The brightest material has a normal visible albedo of about 0.5.

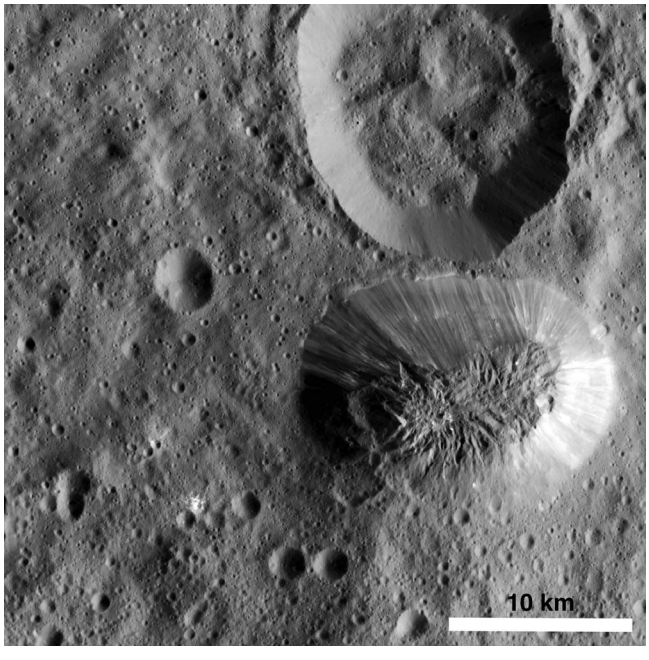

Fig. 2. Panchromatic image of Ahuna Mons (316.2°E, 10.5°S) from the low-altitude mapping orbit.

The Herschel Space Observatory detected water vapor around Ceres (*10*), but a search in forward-scattering conditions during the initial highest-altitude polar orbit in April and early May 2015 showed no scattered light due to possible ejected particles. A study of the bright regions on the Ceres surface, over the interval for which surface brightness has been measured with HST and then with Dawn, did not reveal any brightness changes during this period at 30-km scale (*17*). Dawn's instruments are not well suited to the type or level of water vapor reported by Herschel. A search for a detectable exosphere on Ceres using the Cosmic Origins Spectrometer on the HST was also unsuccessful (*29*).

An unexpected detection of energetic charged particles at Ceres may have an exospheric link. Figure 4 shows counts in the Dawn Gamma Ray and Neutron Detector (GRaND) (*30*) at an altitude of 4400 km. Results indicate detection of energetic electrons in the nadir-pointing detector, which has a field of view of close to 2π steradians. The broad peak on 18 to 21 June is a solar proton event. The unusual features are the rapid bursts seen on three successive orbits. These spikes in the counting rates are caused by the electromagnetic (bremsstrahlung) radiation produced by energetic electrons of many tens of kilo–electron volts impinging on the spacecraft. As shown in the supplementary materials, the locations of the observations on each of the three orbits over a 7-day period are plotted on a solar-oriented coordinate system. Alternatively, no ordering is seen if planetary longitude is used. Other energetic particle events have been detected during cruise, Vesta, and Ceres encounters; however, there were no accompanying electron bursts like those seen in Fig. 4. Similar electron bursts are seen by detectors on spacecraft in high-Earth orbit in the solar wind when the magnetic field at the spacecraft lies tangent to the surface of the bow shock. These signals are attributed to rapid acceleration of electrons to very high energies (*31*). When the interplanetary field lines are convected through the shock, the electrons orbiting that magnetic field line experience an increasing field strength that, near the point of tangency of the field line and the shock, rapidly accelerates electrons gyrating nearly perpendicular to the magnetic field up to very high energies. This mechanism is called fast Fermi acceleration (*32*, *33*) as it involves a magnetic mirror that moves very rapidly.

There are two ways for Ceres to produce a bow shock in a transient manner lasting ~6 days. First, a weak atmosphere at Ceres consistent with the Herschel observations could have been ionized by the energetic particles in the solar wind, mass loading the solar wind and producing a bow shock as the solar wind was deflected around the mass-loading obstacle. When the solar particle event terminated, the ionization stopped, and this exosphere would gradually disappear. The expected time scale for such a temporary exosphere to disappear is of the order of a week (*34*). A second means of possibly deflecting the solar wind is via the

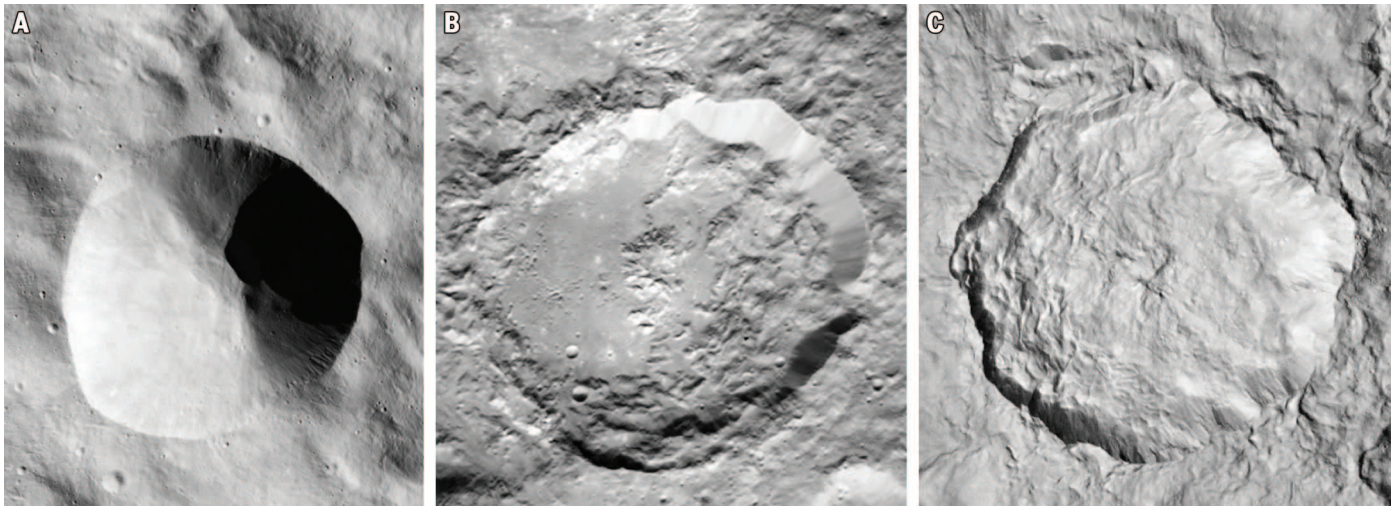

Fig. 3. Comparison of the morphologies of typical fresh craters of similar size. Torpeia crater on Vesta (**A**) is 40-km wide; Ikapati crater on Ceres (**B**) is 48-km wide; Inktomi crater on Saturn's icy moon Rhea (**C**) is 49-km wide.

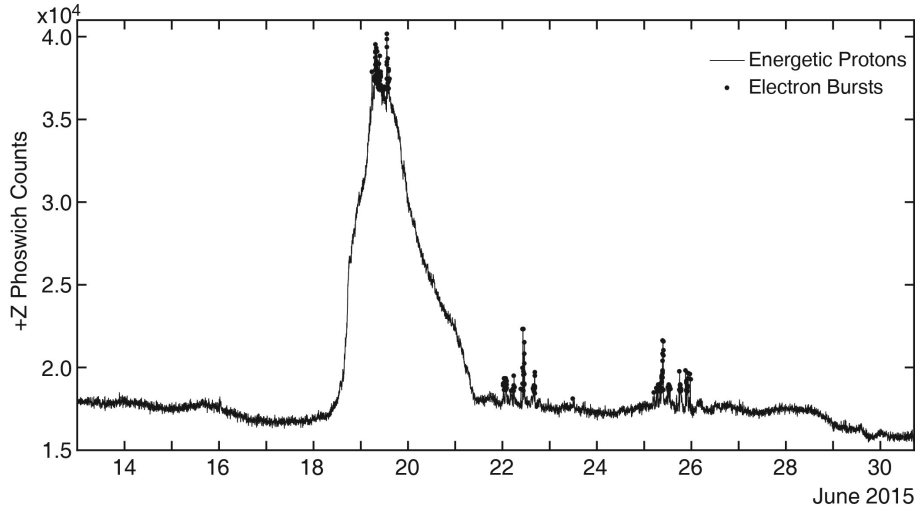

Fig. 4. Gross counts per 210 s measured by the +Z phoswich sensor within the gamma-ray and neutron detector. This sensor is sensitive to bremsstrahlung produced by the interaction of swift electrons with the instrument housing, and to solar energetic protons. The electron bursts were detected while GRaND was pointed toward the hemisphere that contained Ceres. The slowly varying solar proton event on 18 to 21 June and the energetic proton background are designated by the solid line. The electron burst contribution is indicated by the dotted peaks.

magnetic cloud that often accompanies such a solar energetic particle event. If, as has been hypothesized, Ceres is wet inside and the salty mix is electrically conductive, then the magnetic cloud would induce an electric current inside Ceres, creating a magnetic field that would deflect the solar wind. This magnetic barrier would exist until the currents inside Ceres decayed. Such models require electrical conductivities higher than we expect (see supplementary materials), as well as greater conducting shell thicknesses, to reproduce the observed time scales. Thus, we favor the temporary atmosphere explanation, because it reproduces the observed time scales with no assumptions about the conditions internal to Ceres.

REFERENCES AND NOTES

1. C. Peebles, *Asteroids: A History* (Smithsonian Institution Scholarly Press, 2000).
2. C. T. Russell, H. Y. McSween, R. Jaumann, C. A. Raymond, in *Asteroids IV*, P. Michel, F. E. DeMeo, W. F. Bottke, Eds. (Univ. of Arizona Press, 2015), pp. 419–432.
3. A. S. Rivkin *et al.*, *Space Sci. Rev.* **163**, 95–116 (2011).
4. W. J. Webster *et al.*, *Astrophys. J.* **95**, 1263–1268 (1988).
5. P. C. Thomas *et al.*, *Nature* **437**, 224–226 (2005).
6. A. S. Konopliv *et al.*, *Icarus* **211**, 401–428 (2011).
7. T. B. McCord, C. Sotin, *J. Geophys. Res.* **110**, E05009 (2005).
8. J. C. Castillo-Rogez, T. B. McCord, *Icarus* **205**, 443–459 (2010).
9. M. F. A'Hearn, P. D. Feldman, *Icarus* **98**, 54–60 (1992).
10. M. Küppers *et al.*, *Nature* **505**, 525–527 (2014).
11. T. V. V. King, R. N. Clark, W. M. Calvin, D. M. Sherman, R. H. Brown, *Science* **255**, 1551–1553 (1992).
12. R. E. Milliken, A. S. Rivkin, *Nat. Geosci.* **2**, 258–261 (2009).
13. M. C. De Sanctis *et al.*, *Nature* **528**, 241–244 (2015).
14. T. Roatsch *et al.*, *Planet. Space Sci.* **121**, 115–120 (2016).
15. M. A. Chamberlain, M. V. Sykes, G. A. Esquerdo, *Icarus* **188**, 451–456 (2007).
16. J. D. Drummond *et al.*, *Icarus* **236**, 28–37 (2014).
17. J.-Y. Li *et al.*, *Astrophys. J.* **817**, L22 (2016).
18. A. Nathues *et al.*, *Nature* **528**, 237–240 (2015).
19. M. C. De Sanctis *et al.*, *Nature* **536**, 54–57 (2016).
20. E. Ammannito *et al.*, *Science* **353**, aaf4279 (2016).
21. O. Ruesch *et al.*, *Science* **353**, aaf4286 (2016).
22. D. A. Williams *et al.*, *Planet. Space Sci.* **103**, 24–35 (2014).
23. P. Schenk *et al.*, *Science* **336**, 694–697 (2012).
24. D. L. Buczkowski *et al.*, *Science* **353**, aaf4332 (2016).
25. M. E. Bland, *Icarus* **226**, 510–521 (2013).
26. H. Hiesinger *et al.*, *Science* **353**, aaf4759 (2016).
27. W. B. Durham, S. H. Kirby, L. A. Stern, *J. Geophys. Res.* **97**, 20883–20897 (1992).
28. J.-P. Combe *et al.*, *Science* **353**, aaf3010 (2016).

ACKNOWLEDGMENTS

We thank the Dawn team for the development, cruise, orbital insertion, and operations of the Dawn spacecraft at Ceres. C.T.R. is supported by the Discovery Program through contract NNM05AA86C to the University of California, Los Angeles. R.R.F. thanks the Lamont-Doherty Earth Observatory Post-Doctoral Fellowship for support. A portion of this work was performed at the Jet Propulsion Laboratory, California Institute of Technology, under contract with NASA. Dawn's Gamma Ray and Neutron Detector is operated by the Planetary Science Institute under contract with the Jet Propulsion Laboratory, California Institute of Technology (JPL). Dawn data are archived with the NASA Planetary Data System. Framing camera data may be obtained at http://sbn.psi.edu/pds/resource/dwncfc2.html. Spectral data from Visible and Infrared Mapping Spectrometer may be obtained at http://sbn.psi.edu/pds/resource/dwncvir.html. GRaND data may be obtained at http://sbn.psi.edu/pds/resource/dwncgrd.html.

SUPPLEMENTARY MATERIALS

www.sciencemag.org/content/353/6303/1008/suppl/DC1
Supplementary Text
Materials and Methods
Figs. S1 to S6
Table S1
References (*29*–*43*)

4 February 2016; accepted 13 July 2016
10.1126/science.aaf4219

Dawn arrives at Ceres: Exploration of a small, volatile-rich world

C. T. Russell, C. A. Raymond, E. Ammannito, D. L. Buczkowski, M. C. De Sanctis, H. Hiesinger, R. Jaumann, A. S. Konopliv, H. Y. McSween, A. Nathues, R. S. Park, C. M. Pieters, T. H. Prettyman, T. B. McCord, L. A. McFadden, S. Mottola, M. T. Zuber, S. P. Joy, C. Polanskey, M. D. Rayman, J. C. Castillo-Rogez, P. J. Chi, J. P. Combe, A. Ermakov, R. R. Fu, M. Hoffmann, Y. D. Jia, S. D. King, D. J. Lawrence, J.-Y. Li, S. Marchi, F. Preusker, T. Roatsch, O. Ruesch, P. Schenk, M. N. Villarreal and N. Yamashita

Science **353** (6303), 1008-1010.
DOI: 10.1126/science.aaf4219